Supporting Information for:

Surface Charges and Shell Crosslinks Each Play Significant Roles in Mediating Degradation, Biofouling, Cytotoxicity and Immunotoxicity for Polyphosphoester-based Nanoparticles

Mahmoud Elsabahy[1,2†*], Shiyi Zhang[1,3,4†], Fuwu Zhang[1], Zhou J. Deng[3,4], Young H. Lim[1], Hai Wang[1], Persouza Parsamian[1], Paula T. Hammond[3,4] and Karen L. Wooley[1*]

[1]Department of Chemistry, Department of Chemical Engineering, Laboratory for Synthetic-Biologic Interactions, Texas A&M University, P.O. Box 30012, 3255 TAMU, College Station, Texas 77842-3012, United States, [2]Department of Pharmaceutics, Faculty of Pharmacy, Assiut Clinical Center of Nanomedicine, Al-Rajhy Liver Hospital, Assiut University, Assiut, Egypt, [3]David H. Koch Institute for Integrative, Cancer Research, [4]Department of Chemical Engineering, Massachusetts Institute of Technology, Cambridge, MA 02139

† These authors contributed equally to the manuscript

[*] Correspondence to:

mahmoud.elsabahy@chem.tamu.edu, wooley@chem.tamu.edu

EXPERIMENTAL SECTION

Materials

The non-ionic, anionic, cationic and zwitterionic micelles were formed by suspending, independently, four amphiphilic diblock polyphosphoesters into water, which were functionalized from the same parental hydrophobic-functional AB diblock polyphosphoester by "click" type thiol-yne reactions, as reported previously.[1] 3,3'-(ethane-1,2-diylbis(oxy))dipropanoic acid (Bis-dPEG®2-acid) was used as received from Quanta BioDesign, Ltd. (Powell, Ohio). Acetic acid , sodium acetate, 3-morpholinopropane-1-sulfonic acid sodium salt (MOPS), 2,2'-(ethylenedioxy)bis(ethylamine) and 1-[3'-(dimethylamino)propyl]-3-ethylcarbodiimide methiodide (EDCI) were used as received from Sigma-Aldrich Company (St. Louis, MO). Nanopure water (18 MΩ·cm) was acquired by means of a Milli-Q water filtration system, Millipore Corp. (St. Charles, MO). Ultrapure water (Molecular Biology Grade, Fisher BioReagents) was used as received from Thermo Fisher Scientific Inc (Pittsburgh, PA).

Characterization Techniques

Transmission electron microscopy (TEM) was conducted on a Hitachi H-7500 microscope, operating at 100 kV. Samples for TEM measurements were prepared as follows: 4 μL of the dilute solution (with a polymer concentration of 0.1 mg/mL) was deposited onto a carbon-coated copper grid, and after 2 min, the excess of the solution was quickly wicked away with a piece of filter paper. The samples were then negatively stained with 1 *wt*% phosphotungstic acid (PTA) aqueous solution. After 1 min, the excess staining solution was quickly wicked away with a piece of filter paper and the samples were left to dry under ambient conditions overnight. The average diameter of nanoparticles on the TEM grid was obtained by measuring the core domain of 200 sphere particles at different areas of the TEM specimen and the standard deviation was presented as error. Dynamic light scattering (DLS) measurements were conducted using a Delsa Nano C from Beckman Coulter, Inc. (Fullerton, CA)

equipped with a laser diode operating at 658 nm. Scattered light was detected at 165° angle and analyzed using a log correlator over 70 accumulations for a 0.5 mL of sample in a glass size cell (0.9 mL capacity). The photomultiplier aperture and the attenuator were automatically adjusted to obtain a photon counting rate of *ca.* 10 kcps. The calculation of the particle size distribution and distribution averages was performed using CONTIN particle size distribution analysis routines using Delsa Nano 2.31 software. The peak averages of histograms from intensity, volume and number distributions out of 70 accumulations were reported as the average diameter of the particles. All determinations were repeated 10 times. The zeta potential values of the nanoparticles were determined by Delsa Nano C particle analyzer (Beckman Coulter. Fullerton, CA) equipped with a 30 mW dual laser diode (658 nm). The zeta potential of the particles in suspension was obtained by measuring the electrophoretic movement of charged particles under an applied electric field. Scattered light was detected at a 30° angle at 25 °C. The zeta potential was measured at five regions in the flow cell and a weighted mean was calculated. These five measurements were used to correct for electroosmotic flow that was induced in the cell due to the surface charge of the cell wall. All determinations were repeated 6 times.

Table S1. The relative expression of the 23 mouse cytokines following treatment of RAW 264.7 mouse macrophages with anionic PPE-micelles and SCKs, and their degradation products (Deg) at 5 μg/mL for 24 h. The indicated *p* values highlight the significance of differences between the measured concentrations of the treatment and the control, and only cytokines of *p* values less than 0.05 are shown in the table.

Nanoparticle	Induced cytokines	*p* value
Anionic micelles	RANTES	0.04
Anionic SCKs	MCP-1	0.0003
	MIP-1β	0.02
	TNF-α	0.03
Anionic micelles-Deg	MIP-1β	0.01
	MCP-1	0.04
Anionic SCKs-Deg		

Table S2. The relative expression of the 23 mouse cytokines following treatment of RAW 264.7 mouse macrophages with cationic PPE-micelles and SCKs, and their degradation products at 5 μg/mL for 24 h. The indicated *p* values highlight the significance of differences between the measured concentrations of the treatment and the control, and only cytokines of *p* values less than 0.05 are shown in the table.

Nanoparticle	Induced cytokines	*p* value
Cationic micelles	IL-10	0.0002
	IL-5	0.0008
	MCP-1	0.002
	IL-17	0.003
	KC	0.005
	TNF-α	0.006
	G-CSF	0.01
	IL-12(p40)	0.02
	IL-1β	0.02
	IL-3	0.02
	IL-9	0.03
	MIP-1β	0.03
	Eotaxin	0.04
	IL-4	0.04
Cationic SCKs	IL-12(p40)	0.009
	IL-1β	0.009
	IL-10	0.01
	IL-17	0.01
	IFN-γ	0.02
	IL-3	0.02
	TNF-α	0.02
	IL-4	0.03
	IL-5	0.04
	KC	0.04
	MCP-1	0.04
	MIP-1β	0.04
Cationic micelles-Deg		
Cationic SCKs-Deg	MCP-1	0.02

Table S3. The relative expression of the 23 mouse cytokines following treatment of RAW 264.7 mouse macrophages with zwitterionic PPE-micelles and SCKs, and their degradation products at 5 μg/mL for 24 h. The indicated *p* values highlight the significance of differences between the measured concentrations of the treatment and the control, and only cytokines of *p* values less than 0.05 are shown in the table.

Nanoparticle	Induced cytokines	*p* value
Zwitterionic micelles	MCP-1	0.009
	MIP-1α	0.02
	MIP-1β	0.02
	IFN-γ	0.03
	IL-10	0.03
	IL-17	0.04
	IL-5	0.04
Zwitterionic SCKs		
Zwitterionic micelles-Deg		
Zwitterionic SCKs-Deg		

Table S4. The relative expression of the 23 mouse cytokines following treatment of RAW 264.7 mouse macrophages with neutral PPE-micelles and the degradation products of the neutral micelles and the PBYP-*b*-PHP backbone at 5 μg/mL for 24 h. The indicated *p* values highlight the significance of differences between the measured concentrations of the treatment and the control, and only cytokines of *p* values less than 0.05 are shown in the table.

Nanoparticle	Induced cytokines	*p* value
Neutral micelles	MCP-1	0.004
	MIP-1β	0.03
	IL-1α	0.04
Neutral micelles-Deg	MCP-1	0.02
PBYP-*b*-PHP-Deg		

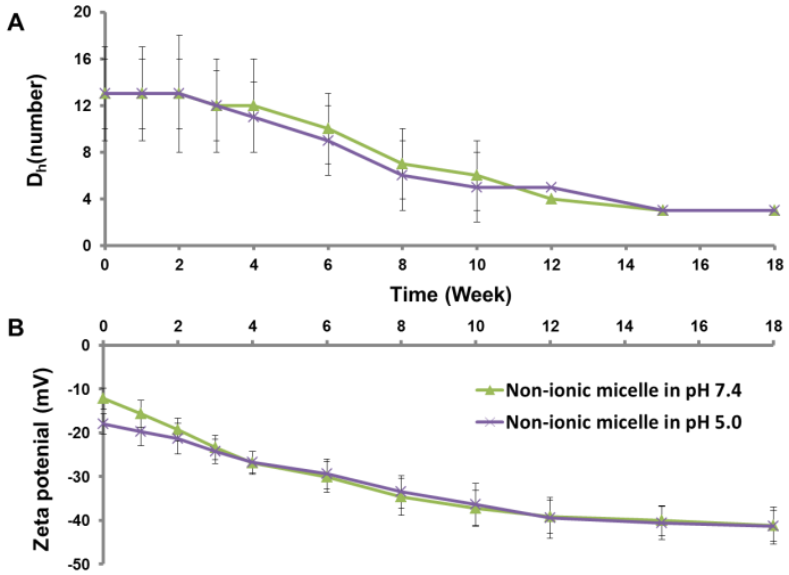

Figure S1. (A) Changes in hydrodynamic diameters by DLS for non-ionic micelle, **1**, as a function of hydrolytic degradation times. (B) Changes in surface charges by zeta potentials for non-ionic micelle, **1,** as a function of hydrolytic degradation times.

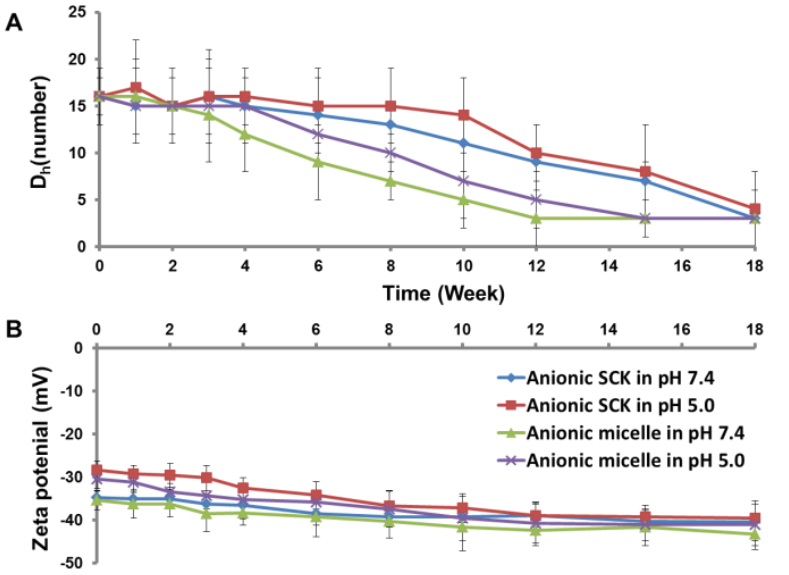

Figure S2. (A) Changes in hydrodynamic diameters by DLS for anionic micelle, **2**, and anionic SCKs, **5**, as a function of hydrolytic degradation times. (B) Changes in surface charges by zeta potentials for anionic micelle, **2**, and anionic SCKs, **5**, as a function of hydrolytic degradation times.

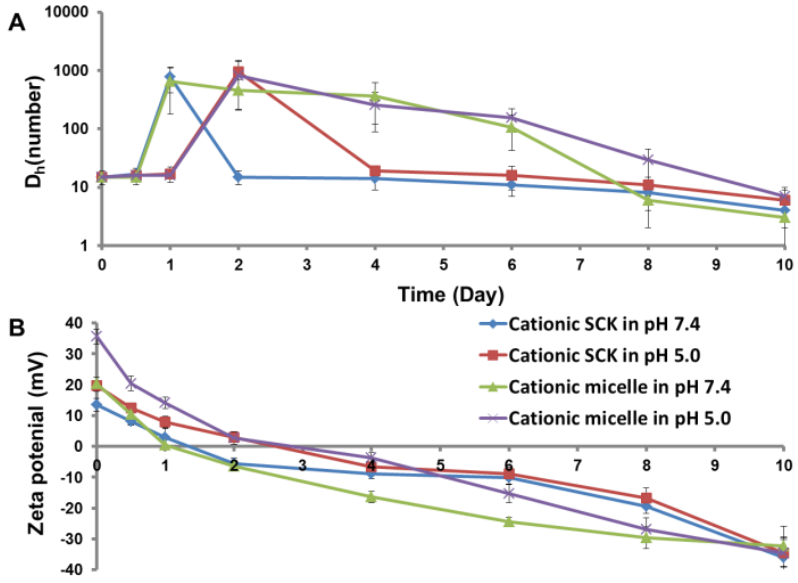

Figure S3. (A) Changes in hydrodynamic diameters by DLS for cationic micelle, **3**, and cationic SCKs, **6**, as a function of hydrolytic degradation times. (B) Changes in surface charges by zeta potentials for cationic micelle, **3**, and cationic SCKs, **6**, as a function of hydrolytic degradation times.

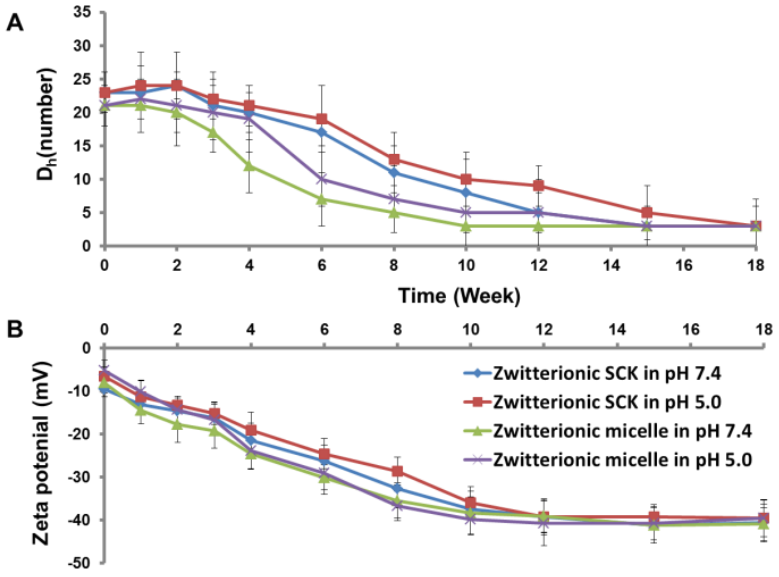

Figure S4. (A) Changes in hydrodynamic diameters by DLS for zwitterionic micelle, **4**, and zwitterionic SCKs, **7**, as a function of hydrolytic degradation times. (B) Changes in surface charges by zeta potentials for zwitterionic micelle, **4**, and zwitterionic SCKs, **7**, as a function of hydrolytic degradation times.

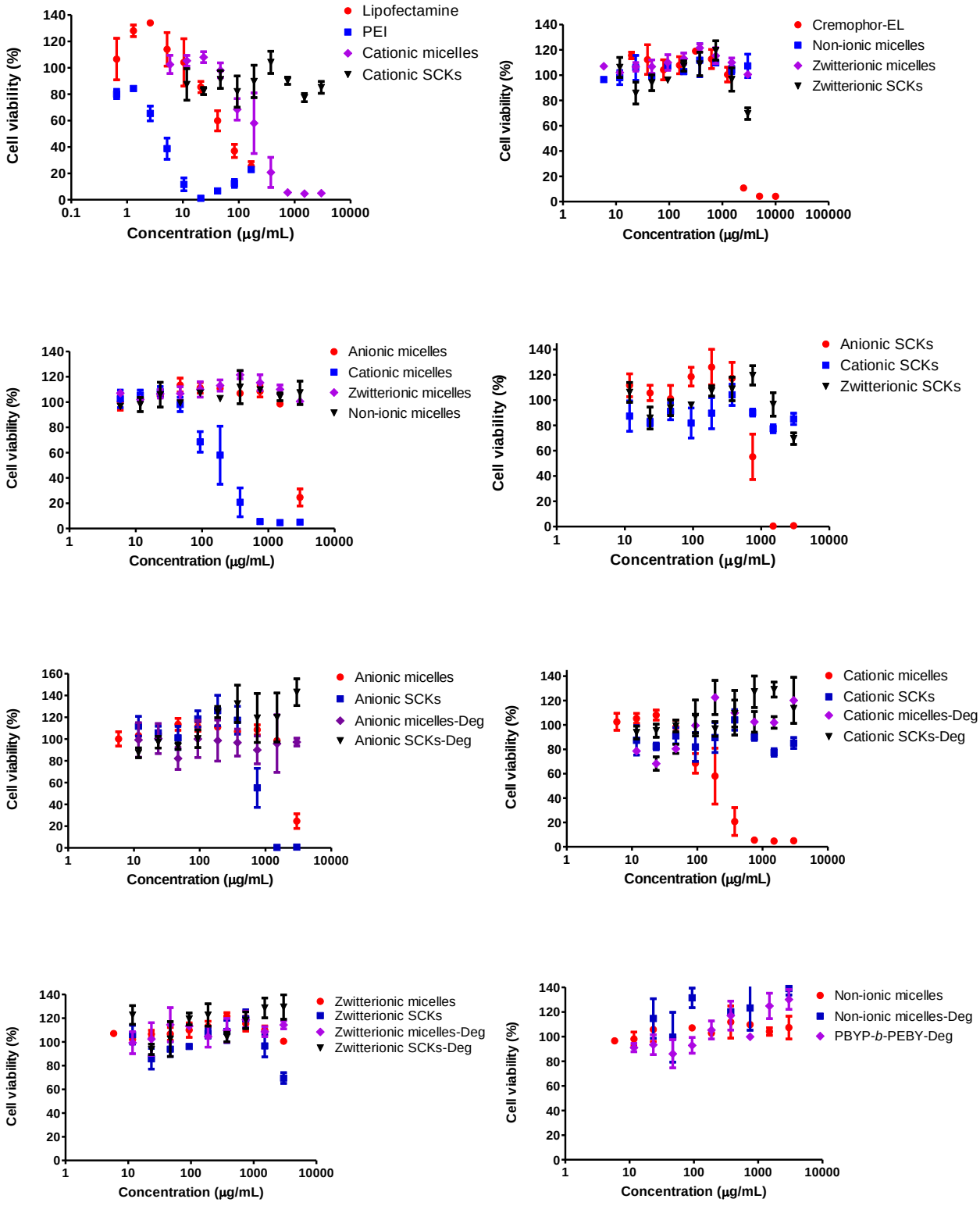

Figure S5. Viability of cells (%) treated with various formulations, including, Lipofectamine, PEI, Cremophor-EL, non-ionic-, zwitterionic-, cationic-, anionic-PPE micelles, zwitterionic-, cationic- and anionic-PPE SCKs, and the degradation products of the various PPE-based nanoparticles (Deg). The graphs present various combinations of nanoparticles and controls to facilitate the comparisons. The values are presented as mean ± SD of at least triplicates.

Reference

1. Zhang, S., Zou, J., Zhang, F., Elsabahy, M., Felder, S.E., Zhu, J., Pochan, D.J. & Wooley, K.L. Rapid and versatile construction of diverse and functional nanostructures derived from a polyphosphoester-based biomimetic block copolymer system. *J. Am. Chem. Soc.* **134**, 18467-18474 (2012).